The EMBO Journal Vol.17 No.9 pp.2451–2462, 1998

Crystal structure of the catalytic subunit of protein kinase CK2 from *Zea mays* at 2.1 Å resolution

Karsten Niefind, Barbara Guerra[1], Lorenzo A.Pinna[2], Olaf-Georg Issinger[1,3] and Dietmar Schomburg[3]

Universität zu Köln, Institut für Biochemie, Zülpicher Strasse 47, D-50674 Köln, Germany, [1]Odense Universitet, Biokemisk Institut, Campusvej 55, DK-5230 Odense, Denmark and [2]Dipartimento di Chimica Biologica, AICR and CNR, Centro di Studio delle Biomembrane, Università di Padova, via G. Colombo 3, I-35121 Padova, Italy

[3]Corresponding authors

CK2α is the catalytic subunit of protein kinase CK2, an acidophilic and constitutively active eukaryotic Ser/Thr kinase involved in cell proliferation. A crystal structure, at 2.1 Å resolution, of recombinant maize CK2α (rmCK2α) in the presence of ATP and Mg^{2+}, shows the enzyme in an active conformation stabilized by interactions of the N-terminal region with the activation segment and with a cluster of basic residues known as the substrate recognition site. The close interaction between the N-terminal region and the activation segment is unique among known protein kinase structures and probably contributes to the constitutively active nature of CK2. The active centre is occupied by a partially disordered ATP molecule with the adenine base attached to a novel binding site of low specificity. This finding explains the observation that CK2, unlike other protein kinases, can use both ATP and GTP as phosphorylating agents.

Keywords: activation segment/co-substrate specificity/ N-terminal region/protein kinase CK2/X-ray crystallography

Introduction

Protein kinase CK2—formerly called casein kinase II or casein kinase 2—is ubiquitously distributed among eukaryotic cells. The enzyme is a Ser/Thr kinase with the specific recognition motif S/TXXD/E (Pinna, 1990), but recent results indicate that it is also able to catalyse tyrosine phosphorylation (Wilson *et al.*, 1997). CK2 has been the subject of several functional and structural studies (for review, see Pinna, 1990; Issinger, 1993; Allende and Allende, 1995). CK2 is composed of four chains ($\alpha_2\beta_2$, $\alpha'_2\beta_2$ or $\alpha\alpha'\beta_2$) making up two catalytic subunits (α and/ or α′) and two regulatory CK2β-subunits. The generation of the tetramer is achieved exclusively by the ability of the β-subunit to form homo- and heterodimers with catalytic subunits, while the two catalytic subunits make no contacts with each other (Gietz *et al.*, 1995). This quaternary structure is so stable that denaturing conditions are necessary for dissociation of CK2.

Despite the stability of the tetramer, the CK2α subunit alone shows catalytic activity. When expressed as a transgene product in mouse lymphocytes, it leads to lymphomas (Seldin and Leder, 1995) and it may be a factor in the regulation of the mitogen-activated protein kinase (MAPK) pathway (Heriché *et al.*, 1997). The CK2 tetramer is known to be involved in cell proliferation (Münstermann *et al.*, 1990; Issinger, 1993), but the biological functions of CK2 and CK2α are not well characterized, although numerous protein substrates have been identified by *in vitro* studies (Meggio *et al.*, 1994; Allende and Allende, 1995).

With respect to biochemistry, three features of CK2 that are unusual among protein kinases raised particular interest in this enzyme and its subunits in the past. (i) Regulation: the physiological regulation of CK2 activity is a source of confusion (Allende and Allende, 1995). The apparent absence of second messengers like cAMP, cGMP or Ca^{2+}, the stability of the CK2 tetramer and the fact that both the tetramer and CK2α alone are catalytically active, make the usual regulatory mechanisms of protein kinases (Johnson *et al.*, 1996) unlikely. The lack of a control mechanism, however, is hardly compatible with the pleiotropic nature of the enzyme and the central role it is believed to play in cellular regulation (Issinger, 1993). (ii) Reduced co-substrate specificity: CK2 and CK2α can use both ATP and GTP as phosphorylating agents (Issinger, 1993; Allende and Allende, 1995). (iii) Substrate specificity: CK2 accepts highly acidic protein substrates; in contrast, most other Ser/Thr kinases are basophilic (Pinna, 1990).

Whereas the acidophilic character of CK2 and its structural base have been investigated thoroughly by mutational studies (Sarno *et al.*, 1996; Vaglio *et al.*, 1996), the crystal structure of a CK2α–ATP complex should help to rationalize the constitutively active nature of the enzyme and its exceptional co-substrate specificity, and possibly yield the first structure-based ideas about the regulatory behaviour of CK2. In this context, the structural environment of the ‘activation segment’ (often called the ‘T-loop’), comprising most parts of subdomains VII and VIII (Hanks and Quinn, 1991), was of special interest, because the critical role of this motif in the regulation of kinase activity is well known (Johnson *et al.*, 1996).

The present study deals with CK2α from *Zea mays*, which is significantly more stable than the human counterpart. A β-subunit of CK2 has not been discovered to date, either in maize or in any other plant. Therefore, it cannot be excluded that, in plants, the α-subunit alone constitutes the active CK2 enzyme. This speculation is supported by the unusually high stability and activity of maize CK2α; human CK2α shows only half of the specific activity of human holo-CK2 (1.2 versus 2.4 U/mg), whereas maize CK2α has a specific activity that is at least as high as the human holoenzyme, and often higher when determined

```
                 7 10        20        30        40        50        60
rmCK2α   ~~~~~MSKAR VYADVNVLRP KEYWDYEALT VQWGEQDDYE VVRKVGRGKY SEVFEGINVN
rhCK2α   MSGPVPSRAR VYTDVNTHRP REYWDYESHV VEWGNQDDYQ LVRKLGRGKY SEVFEAINIT
CDK2     ~~~~~~~~~~ ~~~~~~~~~~ ~~~~~~~~~~ ~~~~~MENFQ KVEKIGEGTY GVVYKARNKL
cAPK     aakkgseqes vkeflakake dflkkwetps QNTAQLDQFD RIKTLGTGSF GRVMLVKHKE
              <--------N-terminal region-------> <---β1-->    <----β2--->

        61        70 72       75        85        95       105      114
rmCK2α   NNEKCIIKIL KPV......K KKKIKREIKI LQNLCGGPNI VKLLDIVRDQ HSKTPSLIFE
rhCK2α   NNEKVVVKIL KPV......K KKKIKREIKI LENLRGGPNI ITLADIVKDP VSRTPALVFE
CDK2     TGEVVALKKI RLDTETEGV. PSTAIREISL LKEL.NHPNI VKLLDVIHTE ..NKLYLVFE
cAPK     SGNHYAMKIL DKQKVVKLKQ IEHTLNEKRI LQAV.NFPFL VKLEFSFKDN ..SNLYMVME
           <---β3--->        <-------αC------->      <--β4-->     <--β5->

       115          124      130       140       150       160      169
rmCK2α   YVNNTDFK.V LYP....TLT DYDIRYYIYE LLKALDYCHS QGIMHRDVKP HNVMIDHELR
rhCK2α   HVNNTDFK.Q LYQ....TLT DYDIRFYMYE ILKALDYCHS MGIMHRDVKP HNVMIDHEHR
CDK2     FLH.QDLKKF MDASALTGIP LPLIKSYLFQ LLQGLAFCHS HRVLHRDLKP QNLLIN.TEG
cAPK     YVAGGEMFSH LRRIG..RFS EPHARFYAAQ IVLTFEYLHS LDLIYRDLKP ENLLID.QQG
              <--αD-->       <----------αE--------->  <β6>      <-β7>
                                                           <cat. loop>

       170          180        190       200       210       220      228
rmCK2α   KLRLIDWGLA EFYHP.GKEY NVRVASRYFK GPELLVDLQD YDYSLDMWSL GCMFAGMIFR
rhCK2α   KLRLIDWGLA EFYHP.GQEY NVRVASRYFK GPELLVDYQM YDYSLDMWSL GCMLASMIFR
CDK2     AIKLADFGLA RAFGVPVRTY THEVVTLWYR APEILLGCKY YSTAVDIWSL GCIFAEMVTR
cAPK     YIQVTDFGFA KRVK..GRTW TL.CGTPEYL APEIILSKG. YNKAVDWWAL GVLIYEMAAG
         <-β8>    <-β9>         <p+1-loop>            <-------αF------->
              <-----activation segment------>

        230        240       250       260       270       280      288
rmCK2α   KEPFFYGHDN HDQLVKIAKV LGTDGLNVYL NKYRIELDPQ LEALVGRHSR KPWLKFMNAD
rhCK2α   KEPFFHGHDN YDQLVRIAKV LGTEDLYDYI DKYNIELDPR FNDILGRHSR KRWERFVNSE
CDK2     R.ALFPGDSE IDQLFRIFRT LGTPDEVVWP G...VTSMPD YKPSFPKWAR QDFSKVVPP.
CAPK     Y.PPFFADQP IQIYEKIVSg kvr....... .......... .......... .....FPSH.
               <------αG------><-----αH---->   <---αI--->      <-αJ->

        290        300       310       315       324   330  334 338
rmCK2α   NQHLVSPEAI DFLDKLLRYD HQERLT.... .ALEAMTHPY F.....QQVR AAENSrtra~
rhCK2α   NQHLVSPEAL DFLDKLLRYD HQSRLT.... .AREAMEHPY FYTVVKDQAR MGSSSmpggs
CDK2     ....LDEDGR SLLSQMLHYD PNKRIS.... .AKAALAHPF F.....QDVT ~~~~~~~~~~
cAPK     ....FSSDLK DLLRNLLQVD LTKRFGNLKN GVNDIKNHKW F.....ATTD WIAIYqrkve
         <-αK-><---αL--->                <-αM->        <----αN--->
```

Fig. 1. Structure-based multiple sequence alignment of rmCK2α with rhCK2α, cAPK and CDK2. The sequences of rhCK2α and cAPK are cut at the termini for reasons of presentation. The alignment was calculated with the GCG-program PILEUP (Wisconsin Sequence Analysis Package, 1994) and, in the case of cAPK and CDK2, subsequently refined in critical regions manually using the least-squares-fit routines of O (Jones *et al.*, 1991). Important positions discussed in the text are printed in bold characters, while regions where neither the sequences nor the structures allow any conclusion concerning topological equivalence are printed with small letters. The numbering of rmCK2α follows that of rhCK2α. The β-sheets and the α-helices from αC to αG are named after their equivalents in cAPK (Knighton *et al.*, 1991).

under optimal assay conditions (O.-G.Issinger, unpublished data). However, these data should be considered as a rough indication, because the activities of CK2α and CK2 depend strongly on the salt concentration (Jakobi and Traugh, 1995), and so they are difficult to compare.

For this study, maize CK2α was produced recombinantly from *Escherichia coli* cells (Dobrowolska *et al.*, 1991). Recombinant maize CK2α (rmCK2α) consists of 332 amino acids (Figure 1). Its amino acid sequence is >60% identical to those of CK2α from other species; in particular, it is 75% identical to the human homologue (rhCK2α) (Dobrowolska *et al.*, 1991) (Figure 1). The main difference between maize and human CK2α is found in the C-terminus, which is ~60 amino acids longer in rhCK2α, but nevertheless rmCK2α can form a stable and fully active CK2 tetramer with human CK2β (Boldyreff *et al.*, 1993). An rmCK2α crystal structure was therefore also expected to be a reasonable model for CK2α in general.

Results

Quality of the final structure model

The rmCK2α structure was solved with crystals that were grown in the presence of ATP and Mg^{2+} (Guerra *et al.*, 1998) and belong to the monoclinic space group C2 with lattice constants of: a = 142.6 Å, b = 61.4 Å, c = 45.4 Å and β = 103.1 Å. The structure was determined with Patterson search techniques (molecular replacement) and refined to final R-factors of 20.5% (R_{work}) for all reflections from 26.1 to 2.1 Å resolution, and reasonable temperature factors (Figure 2A) and stereochemical parameters (Tables I and II). The relatively high R-value can be explained with the inferior quality of the diffraction data set (R_{sym} = 10.6%), which was measured at 4°C with six crystals.

One residue (Pro231) was found with a *cis*-configuration at the peptide bond. Apart from Ala193, all non-glycine residues have 'most favoured' or 'additionally allowed'

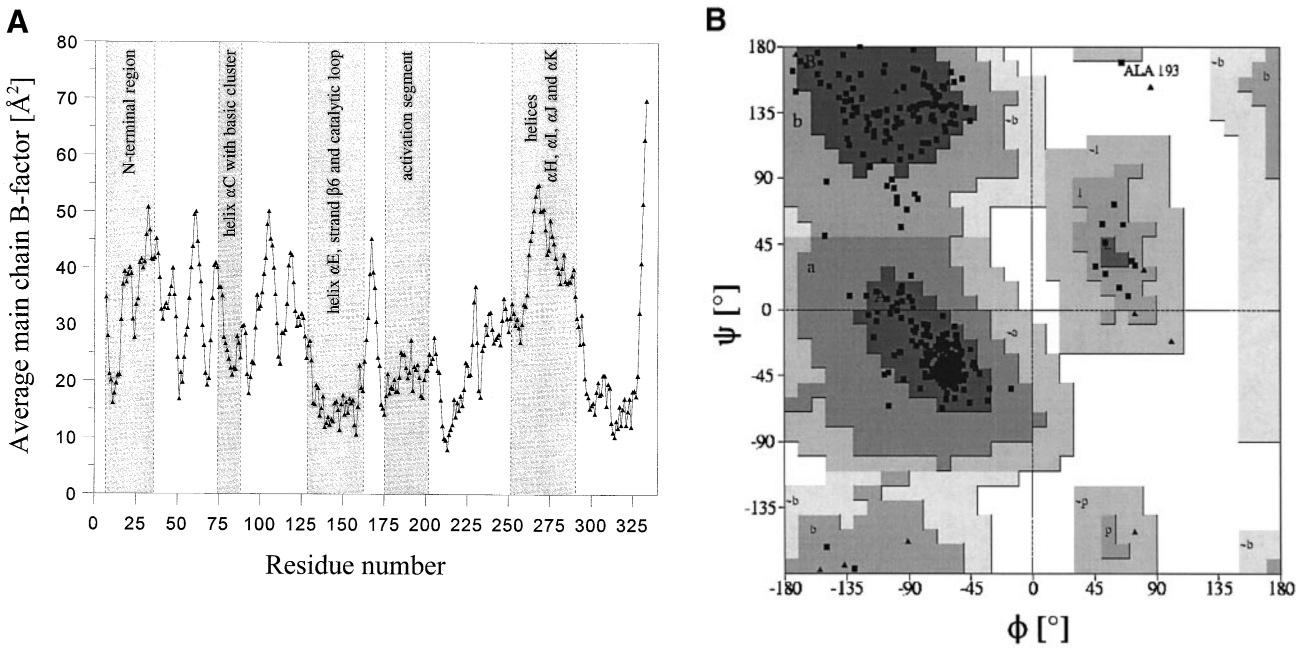

Fig. 2. (**A**) Plot of average main chain temperature factors versus residue number. (**B**) Ramachandran-plot of rmCK2α produced with PROCHECK (Laskowski *et al.*, 1992). Coding: (A, B, L), most favoured regions; (a, b, l, p), additional allowed regions; (~a, ~b, ~l, ~p), generously allowed regions. Glycine residues are shown as triangles.

φ/ψ- combinations (Figure 2B) according to the classification of PROCHECK (Laskowski *et al.*, 1992). The backbone conformation at Ala193 is well defined by electron density (Figure 6C), and so the structural tension at this location is not a refinement artefact. Its possible functional role will be discussed in context of the so-called p+1 loop (Taylor and Radzio-Andzelm, 1994) at the C-terminal side of the activation segment. The quality of the final electron density map is illustrated in Figures 5A, 6A and 6C.

The final rmCK2α model includes 147 water molecules, one molecule of ATP and one magnesium ion. At the N-terminus, Met6 is missing, probably because of post-translational cleavage. With the exception of the last four residues and some polar and solvent exposed side chains, the rmCK2α structure is completely defined by electron density. While the four C-terminal residues were left out of the final model, the disordered side chains were included with idealized conformations and occupancy factors of 0.

Electron density at the co-substrate binding site

In the final stage of refinement, a large, flat piece of residual electron density of significant height remained in the region of the active site (Figure 3A). To explain this density, the complex of cAMP-dependent protein kinase (cAPK) with ATP (Knighton *et al.*, 1991) was superimposed onto the rmCK2α structure. This 3D-fit, the relevant details of which are documented in Figure 3A, showed clearly that the well-described binding sites for adenine and the ribose ring, as observed in several other structures of protein kinase–nucleotide complexes apart from cAPK (Jeffrey *et al.*, 1995; Owen *et al.*, 1995; Xu *et al.*, 1995), were free from significant electron density assignable to ATP. In contrast, the residual density was found at a different position, distant from the classical adenine binding site.

Nevertheless, we attributed the residual density to the

Table I. Characteristic data of the rmCK2α synchrotron data set

No. of crystals used	6
Temperature of data collection	4°C
No. of observations	62 746
No. of observations used after rejections	62 534
No. of independent reflections	21 365
Resolution range (Å)	26.1–2.1
Multiplicity	2.9
Multiplicity for last shell (2.2–2.1 Å)	1.9
Average of (I/σ_I)	8.1
Average of (I/σ_I) for last shell (2.2–2.1 Å)	5.5
Completeness for whole range	95.4%
Completeness for last shell (2.2–2.1 Å)	88.7%
R_{sym} for whole range	10.6%
R_{sym} for last shell (2.2–2.1 Å)	9.6%

$R_{sym}=\Sigma_h\Sigma_j|I_{h,j}-<I_h>|/\Sigma_h\Sigma_jI_{h,j}$, where $I_{h,j}$ is the intensity of the *j*th observation of unique reflection *h*, and $<I_h>$ is the mean intensity of that reflection. Friedel mates were merged in this data set.

Table II. Characteristic data of the rmCK2α crystal structure

Resolution range included in refinement (Å)	2.1–∞
Correlation coefficient F_{obs}/F_{calc} (all reflections)	0.935
R_{free} (5% of all reflections)	27.2%
R_{work} (95% of all reflections)	20.5%
Average B-factor	31.2 Å^2
RMS deviations from	
ideal 1–2 distances (bonds)	0.027 Å
ideal 1–3 distances (angles)	0.040 Å
ideal 1–4 distances (planar groups)	0.054 Å
ideal bond angles	3.6°
Quality of Ramachandran-plot	
Percentage of residues in most favoured[1] regions	87.8%
Percentage of residues in additional allowed[1] regions	11.8%
Mean coordinate error[2] (Å)	0.24

[1]According to the classification in PROCHECK (Laskowski *et al.*, 1992)
[2]Estimated with SIGMAA (Collaborative Computational Project Number 4, 1994)

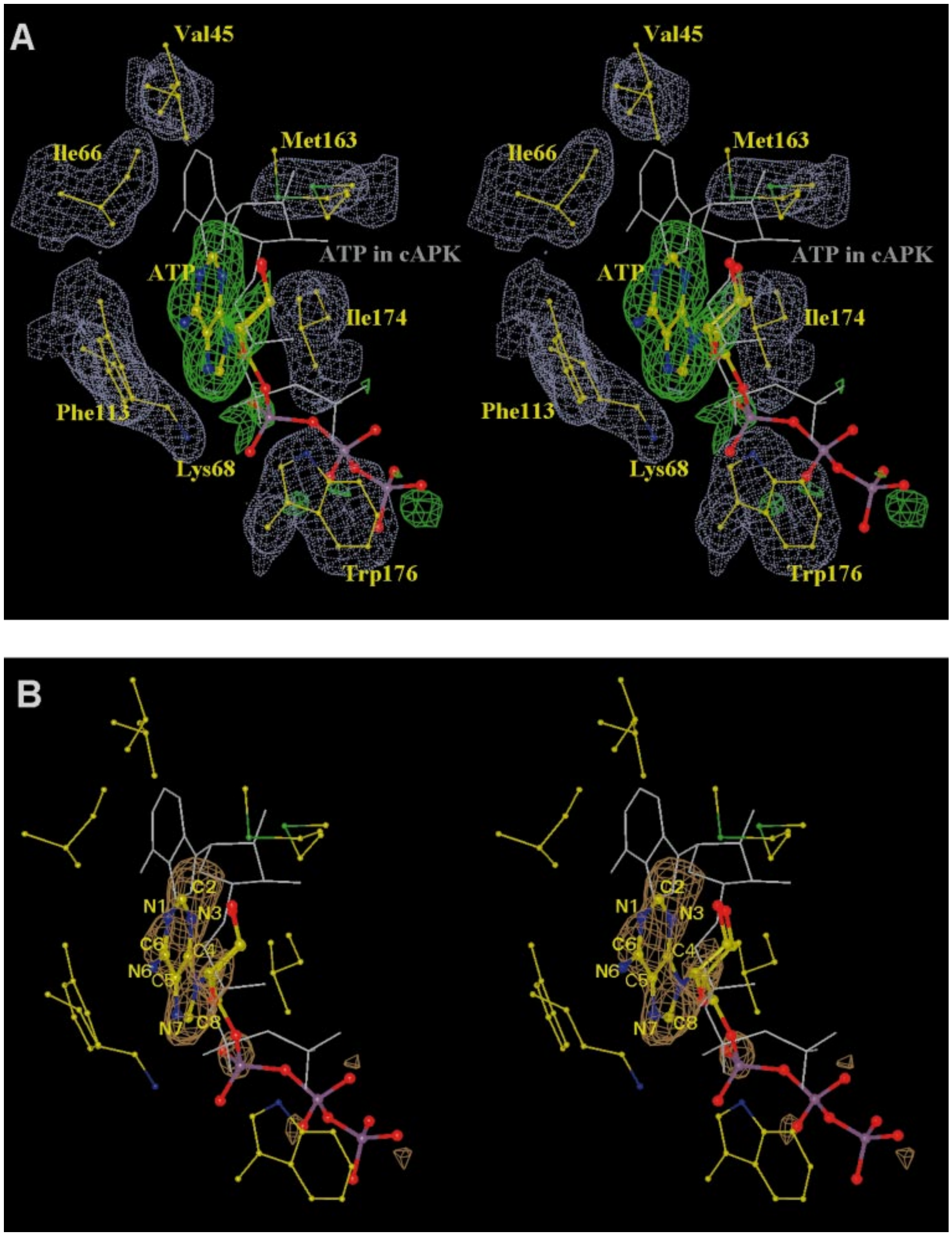

Fig. 3. Stereo illustration of electron density at the nucleotide binding site. Together with ATP, some of the hydrophobic side chains of the environment are drawn. The grey lines show ATP as bound to cAPK (Knighton *et al.*, 1991) after 3D-fit of cAPK and rmCK2α. (**A**) Final ($2F_o$–F_c)-map contoured at 1.1σ. (**B**) (F_o–F_c)-omit map above the 3σ level after two successive 4000 K simulated annealing runs without ATP atoms, using X-PLOR (Brünger, 1992)

adenine moiety of ATP (Figure 3A). This interpretation seemed to be plausible from the beginning, since the exceptional ability of CK2 to accept both ATP and GTP as phosphorylating agents suggested that substantial differences in nucleotide binding in CK2α, compared with other kinases, might be expected. To confirm this further, an omit map (Hodel *et al.*, 1992) was calculated after two successive 4000 K simulated annealing runs without ATP atoms, using X-PLOR (Brünger, 1992). The resulting (F_o–F_c)-omit map (Figure 3B) contained significant electron density that was consistent with the interpretation described.

However, Figure 3A and B also suggests an alternative interpretation: the adenine group could be turned by ~60° around an axis perpendicular to its plane, and shifted towards Met163 so that the density regions that now cover the C8 atom would become free for the ribose ring. This concept would require ATP to be in *syn*-conformation with respect to the torsion angle around the glycosidic bond; it was tested in refinement but finally omitted because of several serious violations of stereochemical constraints.

Hence, while the position of the adenine group in the current rmCK2α model is the most reasonable interpretation of the present experimental data, the rest of the ATP molecule remains undefined. The diffuse electron density in the ribose and triphosphate parts is reflected by average B-factors of 76.7 Å^2 for the ribose atoms and >100 Å^2 for the atoms of the triphosphate group, compared with

38.0 Å for the adenine atoms, so that the conformations of the ribose and the triphosphate group remain unclear. Nevertheless, one magnesium ion was identified by its close coordination with the side chains of Asp175 and Asn161. Its location is equivalent to the low-affinity metal binding site of cAPK, whereas the second metal binding site found in cAPK (Knighton *et al.*, 1991; Bossemeyer *et al.*, 1993) is free from significant electron density.

The partially disordered nature of the ATP molecule is also reflected in the protein environment; in order to fit the corresponding electron density, two alternate side chains had to be assigned to three residues in the neighbourhood of ATP, namely Val45, Val53 and Met163, respectively (Figures 3A and 7).

Discussion

General description of the rmCK2α structure

The global structure of rmCK2α is a variant of the common bilobal architecture of protein kinases (Figure 4A), with a β-rich N-terminal domain, an α-helical C-terminal domain, and the active site in the cleft between them. The N-terminal lobe ends at Asn117 and comprises the β-strands 1–5 and helix αC, while the rest of the molecule belongs to the C-terminal lobe (Figure 1). The molecule has the approximate shape of a bean, with dimensions of about 67, 50 and 42 Å in the directions of the principal axes.

RmCK2α is found in an active conformation. From previous studies with homologous Ser/Thr kinases, an active conformation of such an enzyme is characterized by at least two necessary conditions at a structural level. (i) The activation segment, spanning Asp175 to Glu201 in CK2α, must be folded such that free access for substrate and co-substrate molecules to the active site is possible. This point was demonstrated most impressively in the case of human cyclin-dependent kinase 2 (CDK2). CDK2 as an isolated molecule was found to adopt an inactive state with the activation segment blocking the active site (De Bondt *et al.*, 1993) (Figure 4C), while it exists with an open activation-segment conformation when complexed with a cyclin A fragment (Jeffrey *et al.*, 1995). (ii) The initial part of helix αC, which is critical for substrate recognition in protein kinases (Pinna and Ruzzene, 1996), must be properly aligned towards the active site. In the case of CDK2, this is achieved by interactions with cyclin A (Jeffrey *et al.*, 1995) (Figures 4C and 5B). In CK2α, a highly conserved cluster of preferentially basic residues (K^{74}KKKIKREIK^{83}) (Figure 1) is typical for this zone.

In addition to these two conditions, the orientation of the two lobes relative to each other, and possible ligand-induced inter-lobal displacements, were suggested to be functionally important (Zheng *et al.*, 1993; Helms and McCammon, 1997). A detailed description of two distinct conformational states, one with an open and another with a closed active-site cleft (Figure 4B), was given by Zheng *et al.* (1993) for the catalytic subunit of porcine cAPK. In that particular case, the closed conformation corresponds to a ternary complex, while the open state was observed with the apoenzyme and with a binary complex with a peptide inhibitor. A functional interpretation of this finding, characterizing the open state as active and the closed state as inactive, was given, but it was ambiguous, for comparisons with recombinant murine cAPK showed that the opening state of the active-site cleft in a crystalline environment is likely to be determined by crystal packing constraints (Zheng *et al.*, 1993).

Conforming to the constitutively active nature of CK2, rmCK2α is found in an active state with respect to each of these three aspects. Instead of cyclin A as is the case for CDK2, here it is the N-terminal region (Ser7 to Gln36, Figure 1) which seems to have a key function in the stabilization of this conformation. The N-terminal region links the two lobes of rmCK2α crossing the catalytic cleft and forming well-defined contacts, both with the activation segment and with the basic recognition cluster (Figures 4A, 5A and 6A). The probable key role of the N-terminal region will be discussed further below and will be illustrated in more detail.

Secondary structure

With respect to secondary structure (the assignment of α-helices and β-sheets is shown in Figures 1 and 4A), rmCK2α closely resembles cAPK with four remarkable exceptions. (i) The long N-terminal helix A of cAPK (Figure 4B), which is especially well characterized in non-recombinant porcine cAPK (Zheng *et al.*, 1993), is missing. While it is true that the N-terminal region of rmCK2α possesses short α-helical motifs, its structure is, on the whole, adapted to form an interface with the activation segment (Figures 4A, 4B and 6A). In this way, the N-terminal region itself is stabilized and well defined by electron density, in contrast with some comparable structures of cAPK and protein kinase CK1 (Knighton *et al.*, 1991; Bossemeyer *et al.*, 1993; Xu *et al.*, 1995). (ii) RmCK2α is six residues shorter than cAPK at the region between strand β3 and helix αC, and lacks helix αB completely (Figure 4A and B). It must be assumed that this structural difference is functionally significant, because it concerns a region important for substrate recognition in protein kinases (Pinna and Ruzzene, 1996). In rmCK2α, this region contains the previously mentioned, almost invariant cluster of basic residues (K^{74}KKKIKREIK^{83}), which mainly determines the acidophilic character of the enzyme and possibly interacts with CK2β (Sarno *et al.*, 1996). (iii) In rmCK2α, the helix αD is four residues shorter at its N-terminal end than in cAPK, and has a significantly different direction to cAPK (Figure 4B) and CDK2 (Figure 4C). In this region, a functionally important residue is located; in cAPK, the side chain of Glu127 is a recognition site for the peptide substrate and simultaneously serves as a hydrogen-bonding anchor for the ribose moiety of ATP (Knighton *et al.*, 1991). In rmCK2α, a similar ribose anchor is missing in accordance with the decreased length and altered orientation of helix αD. Possible consequences of this fact are discussed in the context of the active site. (iv) Close to the C-terminus, rmCK2α is 37 residues longer than cAPK and contains four additional α-helices (αH–αK) (Figures 1 and 4B), characterized by conspicuously high temperature factors (Figure 2A). A structure–function relationship correlated with this difference is not obvious at the moment.

The lysine-rich cluster

As indicated in Figure 1, the central part of the lysine-rich cluster K^{74}KKKIKREIK^{83} can be structurally aligned

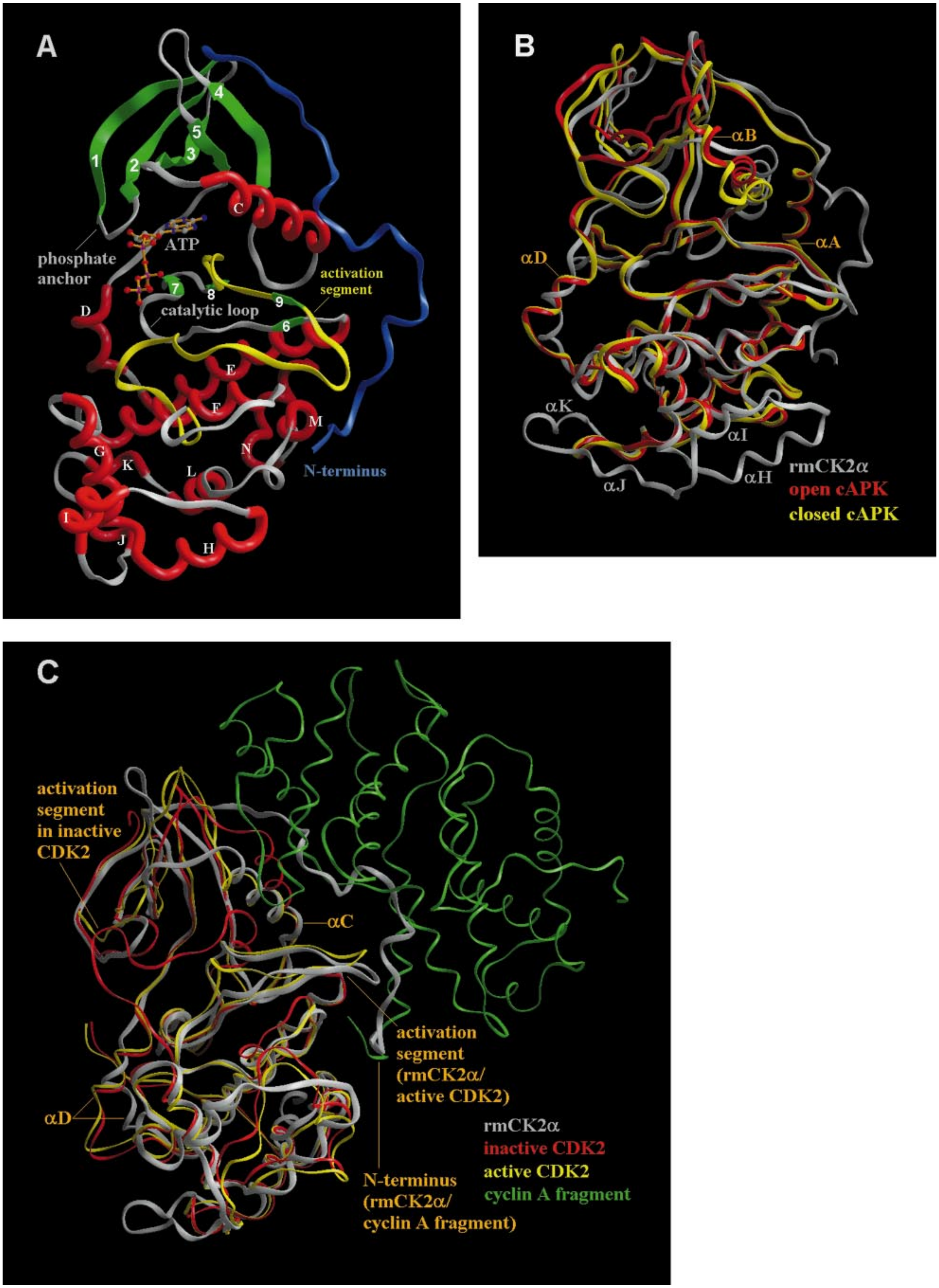

Fig. 4. (**A**) Global view of rmCK2α. To make the contact visible between the N-terminal region (blue) and activation segment (yellow), the molecule was rotated by 90° around the *y*-axis compared with the common view of protein kinases (Knighton *et al.*, 1991). The position of the active site is marked by the bound ATP molecule. The names of the α-helices (red) and the β-sheets (green) are defined in Figure 1.
(**B**) Superposition of rmCK2α (grey), the open, inactive form of cAPK (red) and the closed, active form of cAPK (yellow). The designations of helices αA and αB, which are absent in rmCK2α, refer to cAPK; conversely, αH, αI, αJ and αK refer only to rmCK2α. The long C-terminal tail of cAPK was left out of this figure for reasons of presentation. (**C**) Superpositon of rmCK2α (grey), inactive CDK2 (red) and (partially) active CDK2 (yellow) bound to a fragment of cyclin A (green).

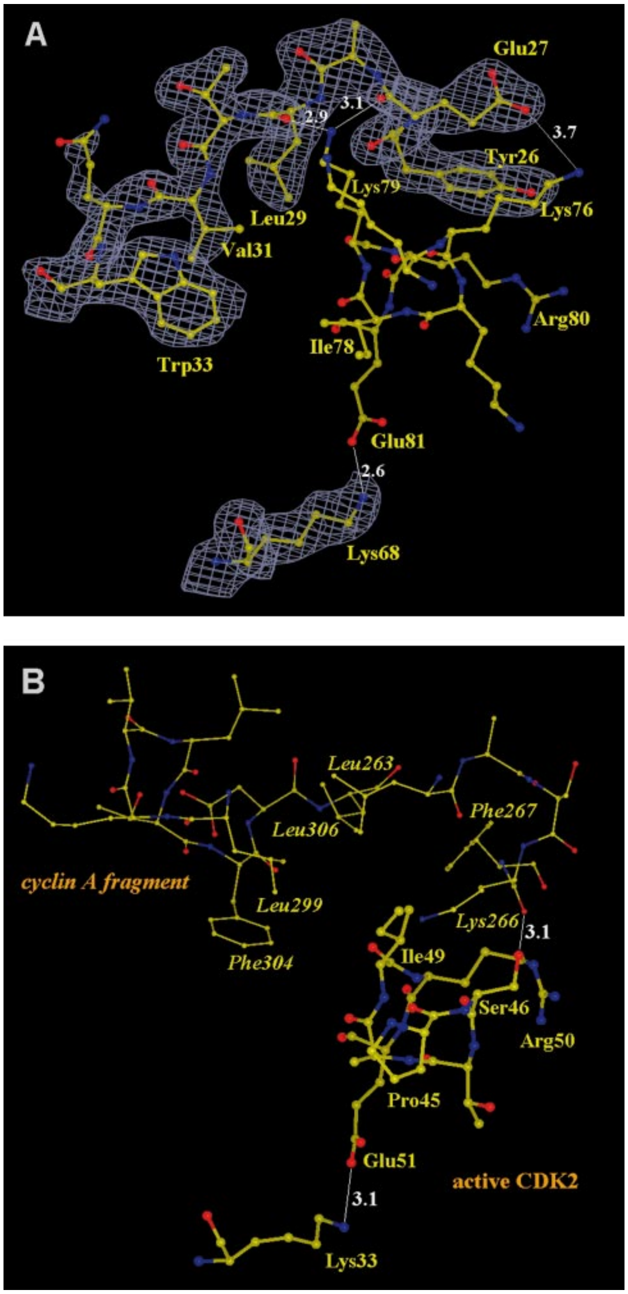

Fig. 5. The basic cluster of rmCK2α in comparison with the PSTAIRE-helix of active CDK2. (**A**) RmCK2α: the basic cluster in contact with the N-terminal segment and Lys68 as part of the active site; N-terminal segment and Lys68 are covered with ($2F_o$–F_c)-electron density above the 1.1 σ level. (**B**) CDK2: PSTAIRE-helix in contact to the active site (Lys33) and to the cyclin A fragment (thin lines). The distances are given in Å.

to the PSTAIRE motif of CDK2, which is located at the beginning of helix αC and plays a crucial role in cyclin A binding and CDK2 activation (Jeffrey *et al.*, 1995). In CDK2, large changes in the conformation of the PSTAIRE region and in the direction of the complete helix αC are associated with cyclin A binding (Figure 4C). These changes are mainly achieved by the formation of a hydrophobic cluster between Ile49 and various non-polar side chains of cyclin A (Figure 5B), and they are transferred to the active site by a salt bridge between Glu51 and Lys33, which is a key catalytic residue and has to be properly orientated for the catalytic mechanism (Jeffrey *et al.*, 1995).

Interestingly, after global structural alignment of the corresponding molecules, the lysine-rich cluster of rmCK2α fits to the PSTAIRE region of the activated, cyclin A bound form and not to that of the inactive, free form of CDK2. The role of cyclin A is assumed by the N-terminal region: Lys76 is in ionic interaction with Glu27, Ile78 together with Trp33 and Val31 is part of a hydrophobic pocket, and the side chain of Lys79—the topological equivalent of Ile49 of CDK2—is hydrogen-bonded to the carbonyl oxygens of Glu27 and Leu29 (Figure 5A). In this way, the N-terminal region stabilizes the active conformation of helix αC and the lysine-rich cluster with the consequence that Glu81 can form a salt bridge to Lys68. The functional importance of this salt bridge can be seen from the fact that Glu81 and Lys68 are the topological and mechanistic equivalents of Glu51 and Lys33 of CDK2 (Jeffrey *et al.*, 1995).

The activation segment

Contact to the N-terminal region. The N-terminal region of rmCK2α, and the activation segment in an open conformation, stabilize each other by extensive contacts (Figure 6A) so that the activation segment belongs to those parts of the structure with the lowest temperature factors (Figure 2A). This arrangement resembles the situation in the CDK2–cyclin A complex, where the top of the activation segment is closely attached to the N-terminus of the activating cyclin A fragment (Figure 6A) (Jeffrey *et al.*, 1995). At the interface between the N-terminal region and activation segment, an aromatic cluster containing Tyr23, Trp24 and Tyr26 on one side, and Phe181 and His183 on the other, is especially conspicuous. Furthermore, strong hydrogen bonds are found connecting Ala9-N with Tyr182-OH, Asn16-ND2 with Tyr182-O and Tyr26-OH with Glu180-OE2. This hydrogen bonding network is further strengthened by some well-defined water molecules, which are presumably essential components of the interface (Figure 6A).

All those residues—both in the N-terminal region and in the activation segment—are highly conserved among CK2α from different species, but not among protein kinases in general (Figure 1) (Hanks and Quinn, 1991; Allende and Allende, 1995). In particular, the sequence motif $L^{173}IDWGLAEFYH^{184}$ is an invariant fingerprint pattern for CK2α: a sequence search using GCG (Wisconsin Sequence Analysis Package, 1994) against the SWISS-PROT database (release 35.0) (Bairoch and Boeckmann, 1992) yielded 18 entries with 100% sequence identity belonging exclusively to CK2α chains, while the next hit with 75% identity, and all following hits, were not CK2α proteins.

The exceptional Trp176. The activation segment begins with a loop that joins the strands β8 and β9 and contains the sequence motif 'DFG' in nearly all kinases (Hanks and Quinn, 1991). CK2α is the only known exception: here, the central phenylalanine is replaced by a tryptophan (Trp176, Figure 1), which had therefore attracted attention in the past in site-directed mutagenesis studies (Jakobi and Traugh, 1992, 1995). Actually, a Trp176Phe mutant

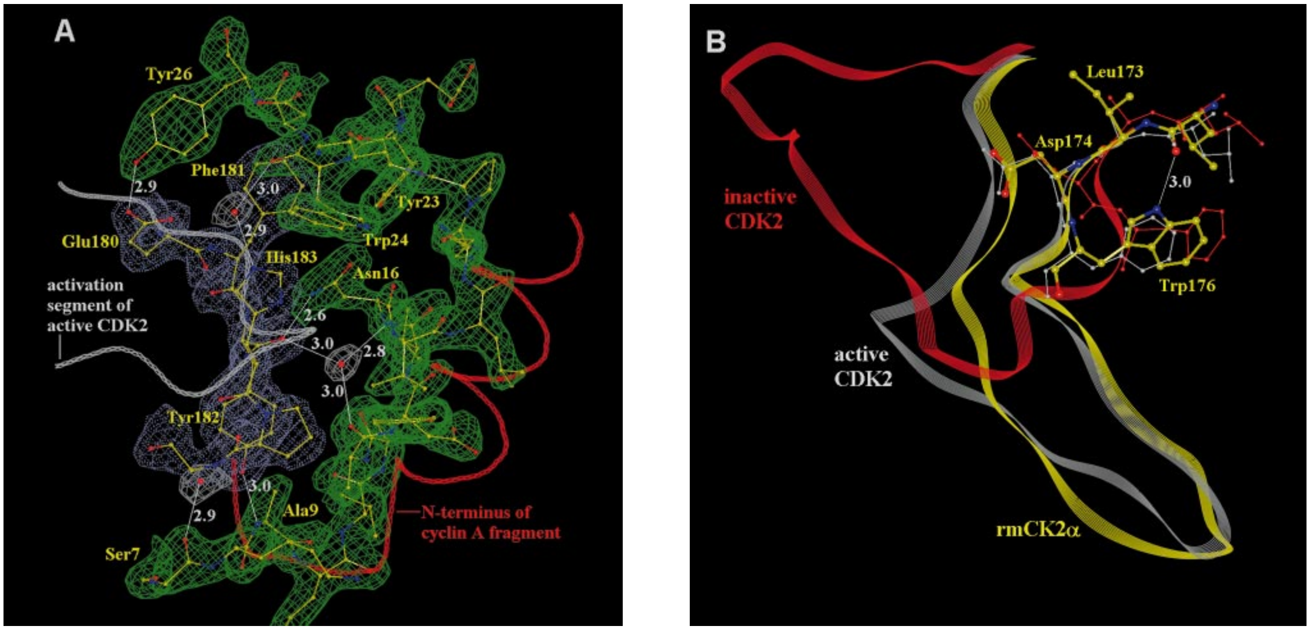

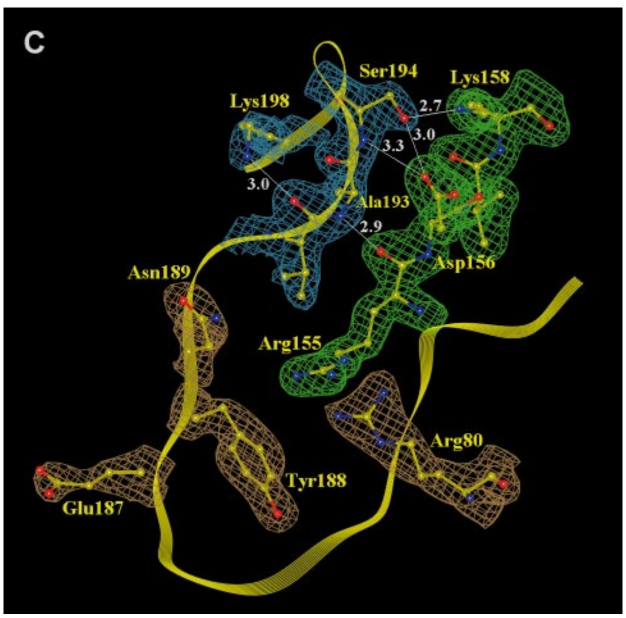

Fig. 6. Structural interactions of the activation segment. Electron density objects are taken from the final $2F_o$–F_c map contoured above 1.5 σ (A) and 1.7 σ (C). The distances are given in Å. (**A**) Contact between activation segment (blue area) and N-terminal region (green area), in comparison with the situation in the complex of CDK2 (grey trace) and a cyclin A fragment (red trace). Water molecules are covered by grey area. (**B**) The role of Trp176 in the N-terminal region of the activation segment; ribbons: activation segment in CK2α (yellow), inactive CDK2 (red) and active CDK2 (grey). (**C**) Ala193 and Ser194 in the p+1 loop (blue area) in contact to the catalytic loop (green area); yellow ribbon: activation segment; furthermore, some neighbouring residues (brown area) mentioned in the text are drawn.

of human CK2α was shown to be significantly less active than the wild-type enzyme (Jakobi and Traugh, 1992).

In CDK2 (De Bondt *et al.*, 1993; Jeffrey *et al.*, 1995), the phenylalanine of the DFG-motif is the first residue of the N-terminal activation segment to move notably during its transition from the open to the closed state (Figures 4C and 6B). In CK2α, an equivalent motion of Trp176 is improbable because of a hydrogen bond across the β8–β9 joining loop between Trp176-NE1 and Leu173-O (Figure 6B). In this way, the active state of the activation segment is stabilized by an internal constraint in addition to the contact with the N-terminal region.

It should be noticed that the β8–β9 joining loop plays an important role in the catalytic mechanism. It includes, first, the magnesium chelating residue Asp175, the equivalent of which in cAPK presumably functions to orientate the γ-phosphoryl group of the co-substrate properly (Bossemeyer *et al.*, 1993), and, second, Ile174 which is part of the hydrophobic binding pocket for the nucleotide base (Figures 3A and 7). The rmCK2α structure is thus consistent with the observation of Jakobi and Traugh (1995) that an exchange (Trp176Phe) influences not only the activity but also the ability of the enzyme to discriminate between ATP and GTP. Nevertheless, it has not yet been possible to rationalize the kinetic values and their trends (Jakobi and Traugh, 1995) in detail.

The negatively charged regulation site of RD-kinases. In addition to controlling access to the active site, the activation loop was also described as performing a fine-tuning of the catalytic activity in 'RD-kinases' (Johnson *et al.*, 1996), which are characterized by an arginine preceding the invariant aspartate in the catalytic loop (Figure 1). A salt bridge from that arginine to a negative charge at the position corresponding to Thr197 of cAPK

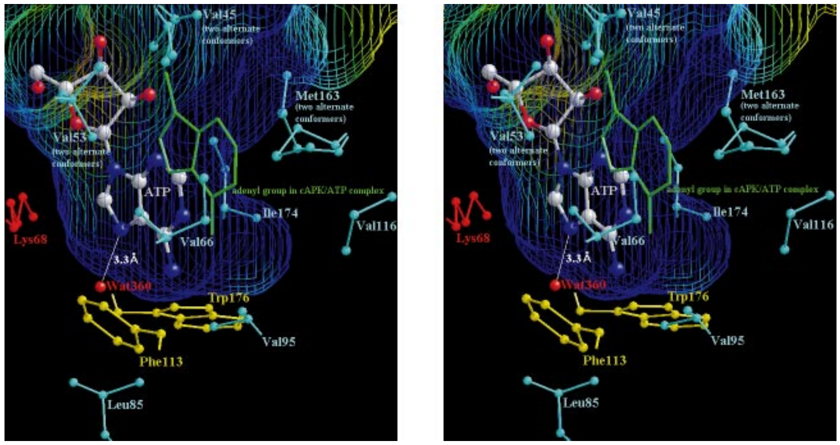

Fig. 7. Stereo illustration of the adenine moiety in the hydrophobic purine binding pocket surrounded by the non-polar side chains contributing to the hydrophobic character. The net marks the hydrophobic surface of the protein matrix including water, with the intensity of the blue colour as an indicator of hydrophobicity. This surface was calculated with BRAGI (Schomburg and Reichelt, 1988). For comparison, the adenine moiety of cAPK-bound ATP is drawn (green) after global 3D-fit of the cAPK/ATP complex on rmCK2α.

is supposed to realign the important residues in the active site (Johnson *et al.*, 1996). The known CK2 kinases are also RD-kinases (Arg155Asp156) (Figure 1), but in the rmCK2α structure, a conserved asparagine (Asn189) is spatially—but not necessarily topologically—equivalent to Thr197 of cAPK (Figure 6C). Whether a neighbouring negative side chain (Glu187, Tyr188 after phosphorylation), an external anion as in protein kinase CK1 (Xu *et al.*, 1995) or a negative side chain of CK2β or of a protein substrate compensates for this lack of a negative charge remains an open question. It is conspicuous that the guanidinium group of Arg80, part of the basic cluster and therefore one of the critical determinants of substrate specificity in CK2 (Sarno *et al.*, 1996), is only 3.6 Å away from the side chain of Arg155 (Figure 6C), thereby establishing a suitable binding site for acidic side chains of peptide substrate or inhibitor molecules.

The p+1 loop. The C-terminal region of the activation segment is known as the 'p+1 loop' because in cAPK it has been shown to interact with the hydrophobic residue following the phosphorylation site of most cAPK substrates (Taylor and Radzio-Andzelm, 1994). In CK2, the importance of the three basic residues of the p+1 loop Arg191, Arg195 and Lys198 for substrate recognition was revealed by mutational studies (Sarno *et al.*, 1996).

In addition to those results, the rmCK2α structure suggests a critical function for Ala193 and in particular for Ser194, which are hydrogen-bonded to essential catalytic loop residues, namely the catalytic base Asp156 and to Lys158, the latter being a candidate for stabilizing the transition state of the γ-phosphoryl group (Bossemeyer *et al.*, 1993) (Figure 6C). Ala193 is, with C_α-torsion angles of 65.1° (φ) and 169.0° (ψ), the only residue of rmCK2α in a disallowed region of the Ramachandran plot (Figure 2B), and hence a place of substantial structural tension in the backbone. This main chain conformation is stabilized by strong hydrogen bonds and is well defined by electron density (Figure 6C). As the position topologically equivalent to Ala193 is occupied by a structurally more variable glycine in most other protein kinases (Hanks and Quinn, 1991), this feature is specific for CK2. It is possible that functionally important structural changes in the activation segment, with effects on Ala193, Ser194 and their hydrogen bonding partners, are influenced by forming and releasing the tension at Ala193.

Such a speculation about a functional role for this region is supported by recent results from a truncated γ-subunit of rabbit muscle phosphorylase kinase in complex with a peptide substrate (Lowe *et al.*, 1997): the residues 183–185 of this kinase, which are topologically equivalent to Arg191, Val192 and Ala193 of rmCK2α, are involved in substrate binding by formation of a short anti-parallel β-sheet with the peptide backbone.

The active site

General considerations. The active site of rmCK2α is quite similar to those of the closed form of cAPK and of CDK2 bound to cyclin A. To stress this point, rmCK2α was fitted globally to these two homologues with the 'lsq_improve' option of 'O' (Jones *et al.*, 1991); afterwards, RMS deviations for 176 backbone atoms of the relevant catalytic elements from both lobes, the phosphate anchor (Gly46 to Val53), the basic cluster (Lys75 to Lys83), the catalytic loop (Arg155 to Asn161) and the activation segment (Leu173 to His183 and Ala193 to Glu201), were calculated. This led to values of 1.2 Å with respect to porcine cAPK in closed form (Bossemeyer *et al.*, 1993) and of 1.6 Å with regard to cyclin A bound CDK2 (Jeffrey *et al.*, 1995). For comparison, the value was 2.2 Å with respect to open cAPK (Zheng *et al.*, 1993; Brookhaven code 1CMK).

Against the background of these similarities, the model of the catalytic mechanism in cAPK (Bossemeyer *et al.*, 1993; Zheng *et al.*, 1993) and in CDK2 (Jeffrey *et al.*, 1995) should, in general, be applicable for rmCK2α, although the diffuse character of the electron density in the triphosphate region of ATP and the absence of a peptide substrate or inhibitor allows no detailed mechanistic discussion for rmCK2α itself. Furthermore, some special features of CK2α function concerning co-substrate specificity can be concluded from significant structural differences compared with other kinases.

The purine binding site. What are the structural reasons for the exceptional ability of CK2 to utilize both ATP and

GTP as co-substrate? Normally, the ATP-binding site is a highly conserved feature in protein kinases, and is characterized by key residues for ribose and triphosphate fixation and for the generation of a hydrophobic adenine binding pocket. For instance, in cAPK, the adenine moiety is flanked by some non-polar side chains and is specifically fixed by three hydrogen bonds: from a backbone nitrogen to the N1-atom, from a backbone oxygen to the N6-amino group and from the side chain of Thr183 to the N7-atom (Knighton *et al.*, 1991; Bossemeyer *et al.*, 1993) (see Figure 3B for atom names). A similar constellation was unlikely in CK2α for reasons of hydrogen bonding potential and availability of space. (i) Because of the unspecific nature of CK2 and CK2α with regard to the co-substrate, the purine binding site should not provide a specific hydrogen bonding pattern fitting only to ATP or GTP. In contrast with ATP the N1-ring nitrogen of GTP is a hydrogen donor and cannot be fixed by a backbone nitrogen; in typical GTP binding sites, it is hydrogen bonded to an aspartate (Noel *et al.*, 1993). Furthermore, in GTP, the equivalent of the N6 amino group of ATP is a carbonyl oxygen, which cannot form the hydrogen bond to a backbone carbonyl mentioned above for the cAPK–ATP complex. (ii) In cAPK, Ala66 is one of the hydrophobic residues in direct contact with one side of the adenine base. This alanine is highly conserved among protein kinases (Hanks and Quinn, 1991) with the remarkable exception of CK2α, where the equivalent position is occupied by a distinctly larger side chain (Val66 in human and Ile66 in maize CK2α) (Figure 1) significantly restricting the space available for the nucleotide base. Actually, the critical role of position 66 in co-substrate binding and selection was demonstrated by mutational studies (Jakobi and Traugh, 1992).

These two arguments are fully consistent with the electron density maps documented in Figure 3A and B and the interpretation given above. They are further highlighted in Figure 7, which shows two facts clearly. (i) The adenine bound in the classical way would penetrate the molecular surface of the protein matrix and would be in serious sterical conflict with the side chain of Ile66. (ii) The purine binding pocket is formed by several non-polar side chains (see also Figure 3A) and therefore possesses a completely hydrophobic surface without the potential for a specific hydrogen-bonding pattern. Consequently, the hydrogen bond between the N7-atom and the well-defined water molecule Wat360 (Figure 7) is the only observed hydrogen bond of the adenine moiety. Indeed, this H-bond can be formed equivalently by any purine nucleotide. In summary, and in full accord with the behaviour shown, neither sterical constraints of the purine binding site nor a particular hydrogen bonding pattern impose an absolute co-substrate specificity on CK2.

The missing ribose anchor. The conformation of the ribose ring remains unclear. This flexibility is compatible with the fact that no hydrogen bonds to the 2′ and 3′ hydroxyl groups are found. In other kinase–ATP complexes, it is generally a negative side chain (Glu127 in cAPK, Asp86 in CDK2) at the beginning of helix αD that functions as ribose anchor (Figure 8). In CK1, a serine side chain at a topologically equivalent position serves the same purpose (Xu *et al.*, 1995). An equivalent fixation, however, is not

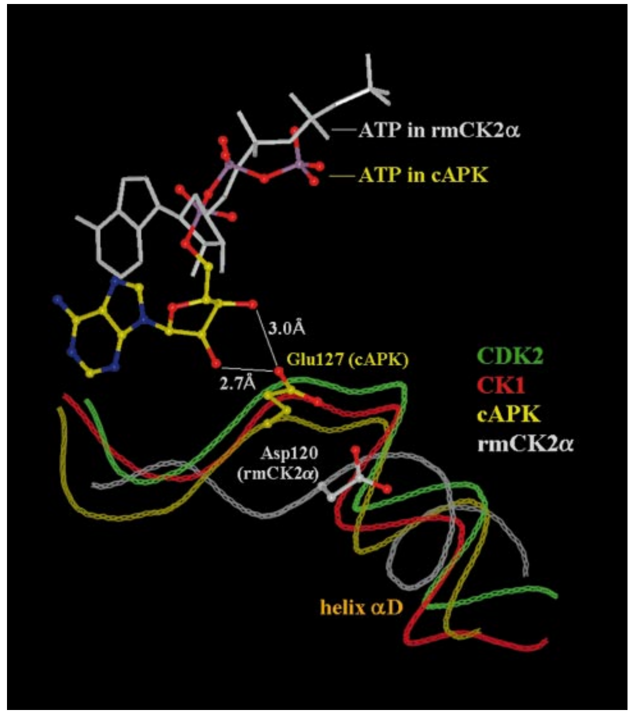

Fig. 8. Helix αD region with ATP ribose anchor in cAPK (yellow), CDK2 (green), protein kinase CK1 (red) and rmCK2α (grey) after global 3D-fits of the structures.

possible in the observed conformation of rmCK2α because the main chain in that region is completely different from that in cAPK, in CDK2 or in CK1 (Figure 8). This refers to length and orientation of helix αD in particular (Figures 4B, C and 8).

An effective ribose binding site, however, might be formed by structural changes in the αD region after binding of CK2β. This idea could at least help to explain some important observations of Jakobi and Traugh (1995). (i) Human CK2α is stimulated *in vitro* by human CK2β, accompanied by an increase in the amount of α-helix, as derived from changes in the corresponding CD spectra. (ii) The increased activity is stable even at salt concentrations of ~250 mM KCl at which CK2α is totally inactivated. It is possible that one of the reasons for these tendencies is the incompleteness of the nucleotide binding site in CK2α leading to loose and unproductive ATP binding. After complex formation with CK2β, backbone changes in the αD region—in particular an extension and rearrangement of helix αD—together with the generation of a ribose anchor might represent an important part of the stimulation and stabilization of activity. This assumption will be checked in the future by a structure determination of a complete CK2 tetramer.

Materials and methods

Crystallization

RmCK2α was expressed in *E.coli* cells, purified and crystallized as described by Guerra *et al.* (1998). Briefly, CK2α was crystallized by vapour diffusion. The reservoirs contained a solution of 25% PEG-4000, 200 mM sodium acetate and 100 mM Tris–HCl pH 8.0. In the crystallization droplets, 3 μl protein stock solution (8 mg/ml CK2α in 500 mM NaCl, 25 mM Tris–HCl, 7 mM 2-mercaptoethanol pH 8.5) were mixed with equal volumes of: first, reservoir; second, 6 mM ATP;

and third, 1.5 mM magnesium chloride. Monoclinic crystals grew within 1 week to a size of ~0.2 mm in each dimension.

Data collection, structure determination and refinement

An X-ray diffraction data set of rmCK2α crystals was collected at 4°C from six different rmCK2α crystals with an MAR imaging plate and synchrotron radiation of 1.1 Å wavelength at the BW6 beamline of DESY (Deutsches Elektronensynchrotron) in Hamburg, Germany. The data were processed with MOSFLM (Leslie *et al.*, 1986) and scaled and merged with SCALA and TRUNCATE from the CCP4 program suite (Collaborative Computational Project, Number 4, 1994). The resulting data set was of acceptable quality from 26.1 to 2.1 Å resolution (Table I). Only four of the six crystals contributed to the whole resolution range; the diffraction patterns of two crystals were collected to only 2.4 Å.

A molecular replacement solution was obtained using the Patterson search routines of X-PLOR 3.1 (Brünger, 1992) and the backbone of CDK2 (De Bondt *et al.*, 1993) as search model. The initial refinement followed the simulated annealing strategy of Brünger *et al.* (1990) as implemented in X-PLOR 3.1 (Brünger, 1992); for manual model building the graphics program O was used (Jones *et al.*, 1991). The final refinement was performed with REFMAC (Collaborative Computational Project, Number 4, 1994) including all data from 26.2 to 2.1 Å without intensity cutoff. The resulting structure is characterized in Table II.

Documentation, interpretation and availability of data

PROCHECK (Laskowski *et al.*, 1992) was used to characterize the stereochemical quality of the final rmCK2α model. The structural figures in this paper were produced with O (Jones *et al.*, 1991) (Figures 3A and B, 5A and B, 6A–C and 8) and BRAGI (Schomburg and Reichelt, 1988) (Figures 4A–C and 7). Sequence database searches, as well as pairwise and multiple sequence alignments, were performed with the routines FASTA, GAP, BESTFIT and PILEUP from GCG (Wisconsin Sequence Analysis Package, 1994).

The final atomic coordinates of rmCK2α, together with the observed structure factor amplitudes, have been deposited in the Brookhaven Protein Data Bank (Bernstein *et al.*, 1977) under the accession No. 1A60.

Acknowledgements

Parts of this work were done at the Gesellschaft für Biotechnologische Forschung (GBF) in Braunschweig, Germany. We thank Dr Gernot Buth for supporting our measurements at the BW6 beamline of DESY, Sabine Weiβflog (GBF) for excellent technical assistance during rmCK2α crystallization, Professor Sung-Hou Kim for sending us the coordinates of CDK2 prior to their release in the Protein Data Bank and Professor Jonathan Howard for carefully reading the manuscript. O.-G.I. and L.A.P. were funded by the Danish Natural Science Research Council, No. 9601695, and the European Biomed2, No. PL 950047.

References

Allende,J.E. and Allende,C.C. (1995) Protein kinase CK2: an enzyme with multiple substrates and a puzzling regulation. *FASEB J.*, **9**, 313–323.

Bairoch,A. and Boeckmann,B. (1992) The SWISS-PROT protein sequence data bank. *Nucleic Acids Res.*, **20**, 2019–2022.

Bernstein,F.C., Koetzle,T.F., Williams,G.J., Meyer,E.E.,Jr, Brice,M.D., Rodgers,J.R., Kennard,O., Shimanouchi,T. and Tasumi,M. (1977) The Protein Data Bank: a computer-based archival file for macromolecular structures. *J. Mol. Biol.*, **112**, 535–542.

Boldyreff,B., Meggio,F., Dobrowolska,G., Pinna,L.A. and Issinger,O.G. (1993) Expression and characterization of a recombinant maize CK-2α subunit. *Biochim. Biophys. Acta*, **1173**, 32–38.

Bossemeyer,D., Engh,R.A., Kinzel,V., Postingl,H. and Huber,R. (1993) Phosphotransferase and substrate binding mechanism of the cAMP-dependent protein kinase catalytic subunit from porcine heart as deduced from the 2.0 Å structure of the complex with Mn^{2+} adenylyl imidodiphosphate and inhibitor peptide PKI (5-24). *EMBO J.*, **12**, 849–859.

Brünger,A.T. (1992) *X-PLOR. Version 3.1. A System for X-ray Crystallography and NMR*. Yale University Press, New Haven, USA.

Brünger,A.T., Krukowski,A. and Erickson, J. (1990) Slow-cooling protocols for crystallographic refinement by simulated annealing. *Acta Cryst.* **A46**, 585–593.

Collaborative Computational Project, Number 4 (1994) *Acta Cryst.*, **D50**, 760–763.

De Bondt,H.L., Rosenblatt,J., Jancarik,J., Jones,H.D., Morgan,D.O. and Kim,S.H. (1993) Crystal structure of cyclin-dependent kinase 2. *Nature*, **363**, 595–602.

Dobrowolska,G., Boldyreff,B. and Issinger,O.G. (1991) Cloning and sequencing of the casein kinase 2α subunit from *Zea Mays. Biochim. Biophys. Acta*, **1129**, 139–140.

Gietz,R.D., Graham,K.C. and Litchfield,D.W. (1995) Interactions between the subunits of casein kinase II. *J. Biol. Chem.*, **270**, 13017–13021.

Guerra,B., Niefind,K., Pinna,L.A., Schomburg,D. and Issinger,O.-G. (1998) Expression, purification and crystallization of the catalytic subunit of protein kinase CK2 from *Zea mays*. *Acta Cryst.*, **D54**, 143–145.

Hanks,S.H. and Quinn,A.M. (1991) Protein kinase catalytic domain sequence database: identification of conserved features of primary structure and classification of family members. *Methods Enzymol.*, **200**, 38–62.

Helms,V. and McCammon,J.A. (1997) Kinase conformations: a computational study of the effect of ligand binding. *Protein Sci.*, **6**, 2336–2343.

Hériché,J.K., Lebrin,F., Rabilloud,T., Leroy,D., Chambaz,E.M. and Goldberg,Y. (1997) Regulation of protein phosphatase 2A by direct interaction with casein kinase 2 alpha. *Science*, **276**, 952–955.

Hodel,A., Kim,S.-H. and Brünger,A.T. (1992) Model bias in macromolecular crystal structures. *Acta Cryst.* **A48**, 851–858.

Issinger,O.G. (1993) Casein kinases: pleiotropic mediators of cellular regulation. *Pharmacol. Ther.*, **59**, 1–30.

Jakobi,R. and Traugh,J.A. (1992) Characterization of the phosphotransferase domain of casein kinase II by site-directed mutagenesis and expression in *Escherichia Coli. J. Biol. Chem.*, **267**, 23894–23902.

Jakobi,R. and Traugh,J.A. (1995) Site-directed mutagenesis and structure/function studies of casein kinase II correlate stimulation of activity by the beta subunit with changes in conformation and ATP/GTP utilization. *Eur. J. Biochem.*, **230**, 1111–1117.

Jeffrey,P.D., Russo,A.A., Polyak,K., Gibbs,E., Hurwitz,J., Massague,J. and Pavletich,N.P. (1995) Mechanism of CDK activation revealed by the structure of a cyclinA–CDK2 complex. *Nature*, **376**, 313–320.

Johnson,L.N., Noble,M.E.M. and Owen, D.J. (1996) Active and inactive protein kinases: structural basis for regulation. *Cell*, **85**, 149–158.

Jones,T.A., Zou,J.Y., Cowan,S.W. and Kjeldgaard,M. (1991) Improved methods for binding protein models in electron density maps and the location of errors in these models. *Acta Cryst.*, **A47**, 110–119.

Knighton,D.R., Zheng,J., Ten Eyck,L.F., Ashford,V.A., Xuong,N.H., Taylor,S.S. and Sowadski,J.M. (1991) Crystal structure of the catalytic subunit of cyclic adenosine monophosphate-dependent protein kinase. *Science*, **253**, 407–414.

Laskowski,R.A., MacArthur,M.W., Moss,D.S. and Thornton,J.M. (1992) PROCHECK: a program to check the stereochemical quality of protein structures. *J. Appl. Cryst.*, **26**, 283–291.

Leslie,A.G.W., Brick,P. and Wonacott,A.J. (1986) An improved program package for the measurement of oscillation photographs. *CCP4 News*, **18**, 33–39.

Lowe,E.D., Noble,M.E.M., Skamnaki,V.T., Oikonomakos,N.G., Owen,D.J. and Johnson,L.N. (1997) The crystal structure of a phosphorylase kinase peptide substrate complex: kinase substrate recognition. *EMBO J.*, **16**, 6646–6658.

Meggio,F., Marin,O. and Pinna,L.A. (1994) Substrate specificity of protein kinase CK2. *Cell. Mol. Biol. Res.*, **40**, 401–409.

Münstermann,U., Fritz,G., Seitz,G., Lu,Y.P., Schneider,H.R. and Issinger,O.G. (1990) Casein kinase II is elevated in solid human tumours and rapidly proliferating non-neoplastic tissue. *Eur. J. Biochem.*, **189**, 251–257.

Noel,J.P., Hamm,H.E. and Sigler,P.B. (1993) The 2.2 Å crystal structure of transducin-α complexed with GTPγS. *Nature*, **366**, 654–663.

Owen,D.J., Noble,M.E.M., Garman, E.F., Papageorgiou,A.C. and Johnson,L.N. (1995) Two structures of the catalytic domain of phosphorylase kinase: an active protein kinase complexed with substrate analogue and product. *Structure*, **3**, 467–482.

Pinna,L.A. (1990) Casein kinase 2: an 'eminence grise' in cellular regulation?. *Biochim. Biophys. Acta*, **1054**, 267–284.

Pinna,L.A. and Ruzzene,M. (1996) How do protein kinases recognize their substrates? *Biochim. Biophys. Acta*, **1314**, 191–225.

Sarno,S., Vaglio,P., Meggio,F., Issinger,O.G. and Pinna,L.A. (1996) Protein kinase CK2 mutants defective in substrate recognition. Purification and kinetic analysis. *J. Biol. Chem.*, **271**, 10595–10601.

Schomburg,D. and Reichelt,J. (1988) BRAGI: a comprehensive protein modeling program system. *J. Mol. Graph.*, **6**, 161–165.

Seldin,D.C. and Leder,P. (1995) Casein kinase IIα transgene-induced murine lymphoma relation to theileriasis in cattle. *Science*, **267**, 894–897.

Taylor,S.S. and Radzio-Andzelm,E. (1994) Three protein kinase structures define a common motif. *Structure*, **2**, 345–355.

Vaglio,P., Sarno,S., Marin,O., Meggio,F., Issinger,O.G. and Pinna,L.A. (1996) Mapping the residues of protein kinase CK2 alpha subunit responsible for responsiveness to polyanionic inhibitors. *FEBS Lett.*, **380**, 25–28.

Wisconsin Sequence Analysis Package, (1994) *Program Manual*. Genetics Computer Group, Inc. University Research Park, 575 Science Drive, Madison, WI 53711, USA.

Wilson,L.K., Dhillon,N., Thorner,J. and Martin,G.S. (1997) Casein kinase II catalyzes tyrosine phosphorylation of the yeast nucleolar immunophilin Fpr3. *J. Biol. Chem.*, **272**, 12961–12967.

Xu,R.M., Carmel,G., Sweet,R.M., Kuret,J. and Cheng,X. (1995) Crystal structure of casein kinase-1, a phosphate-directed protein kinase. *EMBO J.*, **14**, 1015–1023.

Zheng, J., Knighton,D.R., Xuong,N.-H., Taylor,S.S., Sowadski,J.M. and Ten Eyck,L.F. (1993) Crystal structures of the myristylated catalytic subunit of cAMP-dependent protein kinase reveal open and closed conformations. *Protein Sci.*, **2**, 1559–1573.

Received December 2, 1997; revised January 1, 1998; accepted February 24, 1998